

Internal-Field Variations with Temperature for the Two Sublattices of Ordered Fe₃Al and Fe₃Si

MARY BETH STEARNS

Scientific Laboratory, Ford Motor Company, Dearborn, Michigan

(Received 23 October 1967)

Using the Mössbauer technique, the variation of the internal magnetic field with temperature from 4.2°K to about 0.9*T_C* was measured for each sublattice of ordered Fe₃Al and Fe₃Si structures. The variation of the reduced internal field with reduced temperature was observed to be almost identical on all the sublattices. In these alloys, it is expected that the reduced internal field varies in the same manner as the reduced magnetization for each sublattice. Thus, we can compare these measurements with the magnetization curves calculated from molecular-field theory. In this way, we obtain the exchange energies for each sublattice and for the interaction between the two sublattices. The values for the Fe₃Al structure are $J_{AD} = 120 \pm 15^\circ\text{K}$, $J_{AA} = 70 \mp 20^\circ\text{K}$, and $J_{DD} = 7 \mp 5^\circ\text{K}$. These values of the exchange energies are very reasonable, indicating that the molecular-field treatment satisfactorily describes the behavior of these alloys. The success of molecular-field theory is consistent with the view that the ferromagnetic behavior of Fe and these alloys is due to the long-range coupling of the atomic spins by the itinerant *d* electrons.

INTRODUCTION

A SIMPLE, direct way to measure the variation of internal fields at various sites in magnetic systems is provided by Mössbauer-type measurements. Here, we report on measurements of the temperature variation of the internal fields of the Fe atoms on each of the sublattices in Fe₃Al and Fe₃Si structures. Although, in general, the variation of the internal field is not necessarily the same as that of the saturation magnetization; for Fe₃Si, we observe that their behavior is very similar (see Fig. 8 of Ref. 1). We thus assume that they are proportional in this paper; this is discussed in more detail later. We can then compare the measured variation of the internal field for each type site with that expected from the molecular-field treatment (Néel theory of ferrimagnetism).^{2,3} In this case, we have a system whose two sublattices are coupled ferromagnetically with also a ferromagnetic coupling between the sublattices (i.e., all three molecular-field coefficients are positive). We find that the agreement between experiment and theory is very satisfactory, indicating that the ferromagnetic interactions are of long range.

EXPERIMENTAL PROCEDURE

X-ray studies⁴ have shown that the ordered body-centered cubic Fe₃Al(Si) structure consists of two interpenetrating simple-cubic sublattices: one containing mainly Fe atoms (*A* and *C* sites, see Fig. 1) and the other alternating Fe (*D* sites) and Al(Si) atoms (*B* sites). The *A*- and *C*-site atoms (denoted by *A* sites from now on) are surrounded by four Fe and four

Al(Si) nearest-neighbor (nn) atoms. The *D*-site Fe atoms are surrounded by 8-nn Fe atoms.

Table I shows the moments obtained from neutron scattering experiments at room temperature (RT).^{5,6} It also lists the RT internal-field values obtained in these experiments. μ_{Fe} is the moment of pure Fe

TABLE I. Moments and internal fields for the Fe sites in Fe₃Al and Fe₃Si.

		<i>A</i> sites	<i>D</i> sites
Fe ₃ Si	μ	$(0.54 \pm 0.05) \mu_{\text{Fe}}$	$(1.08 \pm 0.03) \mu_{\text{Fe}}$
	H_{int}	$(0.60 \pm 0.01) H_{\text{Fe}}$	$(0.94 \pm 0.01) H_{\text{Fe}}$
Fe ₃ Al	μ	$(0.66 \pm 0.05) \mu_{\text{Fe}}$	$(0.96 \pm 0.05) \mu_{\text{Fe}}$
	H_{int}	$(0.64 \pm 0.01) H_{\text{Fe}}$	$(0.89 \pm 0.01) H_{\text{Fe}}$

($=2.2\mu_B$). H_{Fe} is the internal field of pure Fe ($=330$ kG). No moment was detected on the Al atoms. The experiments on Fe₃Si were performed with a polarized neutron beam, and essentially no moment [$(-0.07 \pm 0.06)\mu_B$] was found on the Si atoms.⁵ We see that the proportionality between moment and internal field is very good for the Fe₃Al system and fair for the Fe₃Si system.

The experimental apparatus used to measure the internal field by the Mössbauer technique has been described previously.⁷ The source was Co⁵⁷ in Pd and the absorbers were the ordered alloys. The Fe₃Si was in powder form while the Fe₃Al was a foil of approximately 0.001-in. thickness. Each absorber was sandwiched between two thin Be plates. The Mössbauer pattern of the Fe₃Si indicated that it was completely ordered. The Fe₃Al sample had 25.5 at.% Al, and its Mössbauer spectra indicated that about 94% of the *B*

¹ M. B. Stearns, Phys. Rev. **129**, 1136 (1963).

² L. Néel, Ann. Phys. (Paris) **18**, 5 (1932); Compt. Rend. **203**, 304 (1936); Ann. Phys. (N. Y.) **3**, 137 (1948).

³ (a) J. S. Smart, Am. J. Phys. **23**, 356 (1955). (b) *Magnetism*, edited by G. T. Rado and H. Suhl (Academic Press Inc., New York, 1963), Vol. III, p. 63.

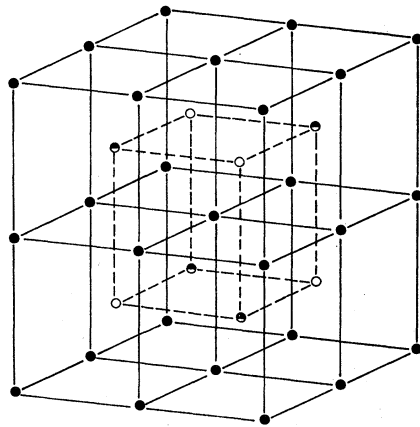
⁴ A. J. Bradley and A. H. Jay, Proc. Roy. Soc. (London) **A136**, 210 (1932).

⁵ A. Paolette and L. Passari, Nuovo Cimento **32**, 25 (1964).

⁶ R. Nathans, T. Pigott, and C. G. Shull, J. Phys. Chem. Solids **6**, 38 (1958).

⁷ M. B. Stearns, Phys. Rev. **147**, 439 (1966).

sites contained Al atoms, which is about the maximum ordering achievable. For temperatures above RT, the absorbers were placed in a small oven containing Be windows. The temperature was controlled with a Pt-Pt-13%Rh thermocouple. No great effort was made to determine the absolute temperatures accurately so they were known to within only 4°K. Below room temperature, the absorbers were mounted on a cold finger of a Dewar. Here, the temperatures of the absorbers were known to about 3°K. The uncertainties in the temperature are well within the circles plotted on Figs. 3 and 4. Figure 2 shows some typical Mössbauer spectra for Fe₃Si. These spectra are clearly composed of two overlapping six-line spectra as shown in Fig. 2 for the 295°K data. The internal fields were determined from the spacing of the outer lines of each of the six-



- Fe atoms - A and C sites
- Fe atoms - D sites
- Al (Si) atoms - B sites

FIG. 1. Unit cell of the ordered Fe₃Al (Si) structure.

line spectra. Before and after each measurement on the alloys, a pure Fe calibration run was made at RT. At each temperature, the data were taken for a long enough time (about 10⁵ counts per channel) so that statistical errors were unimportant. For a discussion of systematic errors due to the electronics, see Ref. 7. The points in Figs. 3 and 4 give the measured reduced internal fields $H(T)/H(0^\circ\text{K})$ as a function of the reduced temperature T/T_C . The Curie temperature T_C used to obtain the reduced temperatures was 713°K for Fe₃Al and 853°K for Fe₃Si.⁸ These values seem the most reliable of those in the literature. However, the conclusions are not dependent upon reasonable variations in the T_C 's. The striking behavior is that, for both alloys, the reduced curves for the A and D sites are essentially the same,

⁸ M. Fallot, Ann. Phys. (Paris) 6, 305 (1936); M. Hansen, Constitution of Binary Alloys (McGraw-Hill Book Co., New York, 1958).

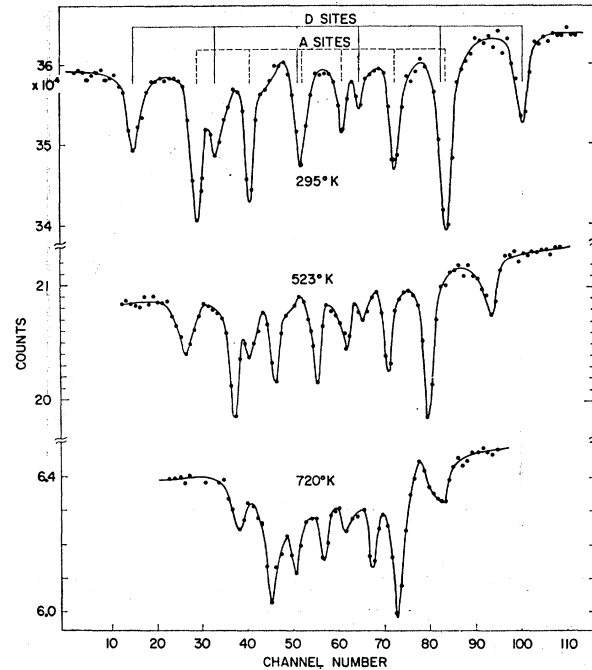


FIG. 2. Typical Mössbauer spectra of Fe₃Si at various temperatures. The internal fields were measured by the distance between the outer peaks of the A and D sites.

with perhaps the D curves being very slightly above the A curves.

COMPARISON WITH THEORY

The internal field is due to the polarization of the s electrons. The dominant contribution is negative and

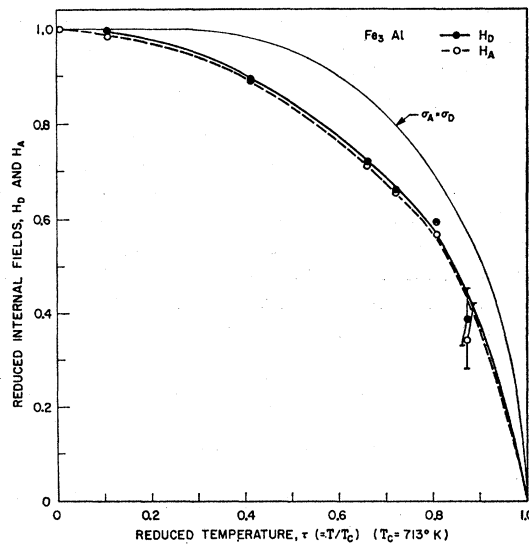


FIG. 3. Measured variations of the reduced internal field with reduced temperature for the two sublattices of Fe₃Al. The curve marked $\sigma_D = \sigma_A$ is a solution of Eqs. (5), where $S_D = 1$ and $S_A = \frac{1}{2}$. When not indicated, the uncertainties in temperature and internal field values are within the data circles shown.

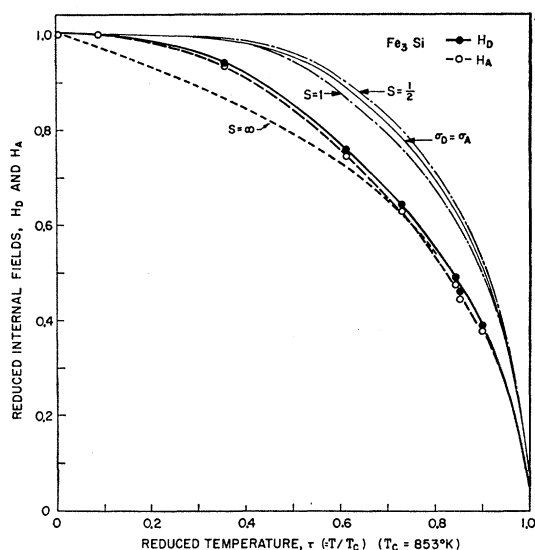


FIG. 4. Measured variation of the reduced internal field with reduced temperature for the two sublattices of Fe_3Si . Also shown are the regular Brillouin functions B_S for $S = \frac{1}{2}$, 1, and ∞ . These are also the solutions of Eqs. (5) when $\sigma_A = \sigma_D$ and $S_A = S_D$. The curve marked $\sigma_D = \sigma_A$ is a solution of Eqs. (5) for $S_D = 1$ and $S_A = \frac{1}{2}$. The uncertainties in temperature and internal-field values are within the shown data circles.

comes from the core (1s, 2s, 3s) electrons. There is also a lesser contribution from the 4s conduction electrons. This contribution, if large enough, could make the measured internal field depend not only on the moment (or magnetization) of its own sublattice, but also on that of the other sublattice. Thus, the reduced internal-field values could depend on the magnetization of both sublattices. We have calculated this effect from the measured polarization curve (Fig. 6 in Ref. 7) for the FeAl alloys, assuming this curve also is applicable to Fe_3Al . We found that the core polarization is indeed overwhelming and that the contribution from the 4s polarization of the sublattice was negligible. This result can be anticipated from Table I where the values of the moments and internal fields are seen to be clearly proportional for Fe_3Al . We are thus justified in assuming that the curves of reduced internal field versus reduced temperature also represent the variation of the reduced magnetizations as a function of reduced temperature.

We shall now compare the measured magnetization curves with those calculated from molecular-field theory. Due to the approximate nature of this theory, we do not expect too close an agreement between the experimental and theoretical curves. The important feature that we wish to consider is that the reduced internal-field dependence of each sublattice on the reduced temperature is essentially the same. We shall closely follow the procedure of Ref. 3(a). The molecular fields which account for the interactions between

magnetic ions are $H_{AA} = \lambda_{AA}M_A$, $H_{AD} = \lambda_{AD}M_D$, $H_{DA} = \lambda_{DA}M_A$, and $H_{DD} = \lambda_{DD}M_D$, where H_{AD} is the molecular field acting on an A atom due to its D neighbors with similar definitions for the other H 's. M_A and M_D are the magnetizations of the A and D sublattices and the λ 's are the Weiss molecular-field coefficients, $\lambda_{AD} = \lambda_{DA}$. In our case, we expect all the λ 's to be positive (i.e., ferromagnetic alignment).

The total fields acting on the A and D atoms with no externally applied fields are

$$\begin{aligned} H_A &= \lambda_{AA}M_A + \lambda_{AD}M_D, \\ H_D &= \lambda_{AD}M_A + \lambda_{DD}M_D. \end{aligned} \quad (1)$$

It is convenient to measure the molecular field coefficients relative to the A - D coefficient so we define

$$\alpha = \lambda_{AA}/\lambda_{AD}, \quad \delta = \lambda_{DD}/\lambda_{AD}. \quad (2)$$

The reduced magnetizations which we identify with the reduced internal fields for each sublattice are given by

$$\begin{aligned} \sigma_A(T) &= M_A(T)/\nu N g \mu_B S_A \\ &= M_A(T)/M_A(0), \\ \sigma_D(T) &= M_D(T)/\lambda N g \mu_B S_D \\ &= M_D(T)/M_D(0), \end{aligned} \quad (3)$$

where $\nu (= \frac{2}{3})$ is the fraction of magnetic ions on the A sites and $\lambda (= \frac{1}{3})$ is the fraction of magnetic ions on the D sites. N is the number of magnetic ions per unit volume, and g is the spectroscopic splitting factor which, in this case, is the same for the two types of atoms. μ_B is the Bohr magneton and S_A , S_D are the spins of the A and D magnetic ions.

According to molecular-field theory, we then obtain

$$\begin{aligned} \sigma_A &= B_{S_A}(g\mu_B S_A H_A/kT), \\ \sigma_D &= B_{S_D}(g\mu_B S_D H_D/kT), \end{aligned} \quad (4)$$

where B_S is the Brillouin function of index S . Substituting in the values of H_A and H_D given by Eq. (1), we thus obtain

$$\begin{aligned} \sigma_A &= B_{S_A}[(3S_A/\tau F)(\nu\alpha S_A\sigma_A + \lambda S_D\sigma_D)], \\ \sigma_D &= B_{S_D}[(3S_D/\tau F)(\lambda\delta S_D\sigma_D + \nu S_A\sigma_A)], \end{aligned} \quad (5)$$

where τ is the reduced temperature T/T_C , and F is given by $F = 3kT_C/Ng^2\mu_B^2\lambda_{AD}$. T_C can be related to the molecular field coefficients^{3(a)} so that F is given by

$$\begin{aligned} F(\lambda, \alpha, \delta, S_A, S_D) &= \frac{1}{2} \{ \lambda\delta S_D(S_D+1) + \nu\alpha S_A(S_A+1) \\ &\quad + [(\lambda\delta S_D(S_D+1) - \nu\alpha S_A(S_A+1))^2 \\ &\quad + 4\nu S_A(S_A+1)S_D(S_D+1)]^{1/2} \}. \end{aligned} \quad (6)$$

The total magnetization σ_T is given by $\sigma_T = \lambda\sigma_D + \nu\sigma_A$. In our case, we have a situation where $S_D \sim 1$ and

$S_A \sim \frac{1}{2}$. However, we find that the conclusions are not dependent on reasonable changes in S_A and S_D . The theory has also been evaluated for $S_A = S_D = \frac{1}{2}$ or 1 (see Fig. 4). These solutions give similar results (the values of α and δ would only be slightly different). Thus, evaluating the Brillouin functions, Eqs. (5) and (6) become

$$\begin{aligned} \sigma_A &= \tanh[(\alpha\sigma_A + \sigma_D)/2\tau F], \\ \sigma_D &= \frac{3}{2} \coth[3(\delta\sigma_D + \sigma_A)/2\tau F] - \frac{1}{2} \coth[(\delta\sigma_D + \sigma_A)/2\tau F], \end{aligned} \tag{5'}$$

$$F = \frac{1}{3} \left\{ \delta + \frac{3}{4}\alpha + [(\delta - \frac{3}{4}\alpha)^2 + 3]^{1/2} \right\}. \tag{6'}$$

For a given α and δ we can solve on a computer for the variation of σ_A and σ_D as a function of τ .

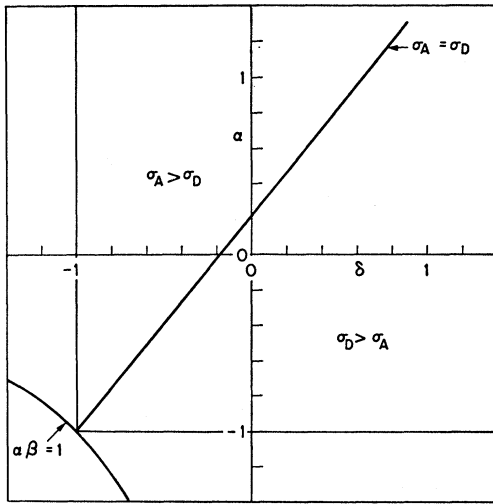


FIG. 5. Various regions of behavior of the solutions to Eqs. (5) as a function of α and δ . See text for a description of the various behaviors.

In the above solution, we have assumed that λ_{AD} is positive, which corresponds to our case. Figure 5 shows general areas of solution for various α 's and δ 's. In the region where both α and δ are less than -1 , the system never becomes spontaneously magnetized at any real temperature. In this region, the large negative molecular-field coefficient of the A or D sublattice successfully opposes the tendency of the A - D interaction to spontaneously magnetize the sublattice. The regions where each sublattice saturates at low temperatures are given by $\delta > -(\nu S_A/\lambda S_D) = -1$ and $\alpha > -(\lambda S_D/\nu S_A) = -1$. Since we have a simple system in which we observe that each sublattice does saturate at low temperature, we are only concerned with this region. In this region, any pair of values (α, δ) which lie on the line marked $\sigma_A = \sigma_D$ give a regular Brillouin behavior. This is shown in Figs. 3 and 4 by the curve marked $\sigma_A = \sigma_D$. Also shown in Fig. 4 are the Brillouin curves for $S_A = S_D = \frac{1}{2}$,

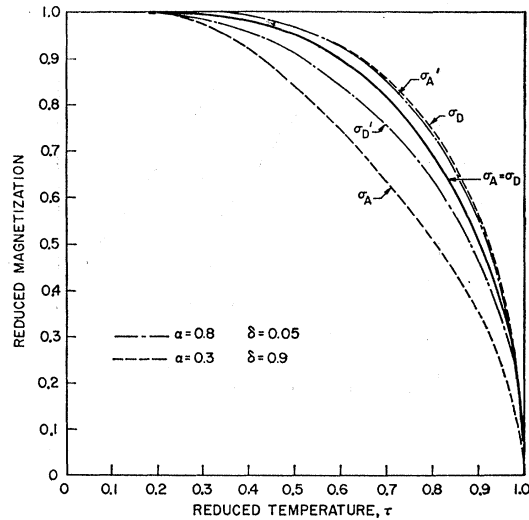


FIG. 6. Some typical variations of the reduced magnetization with reduced temperature as given by Eqs. (5).

1, and ∞ . We see that the curve for $S_A = \frac{1}{2}$, $S_D = 1$ falls between the $S = \frac{1}{2}$ and 1 Brillouin curves as expected. For any other values of α , δ in the region showing saturation, we obtain two separate magnetization curves, one falling above and the other below the $\sigma_A = \sigma_D$ curve. Examples of this behavior are shown in Fig. 6. In the region above and to the left of the line $\sigma_A = \sigma_D$ in Fig. 5, we find $\sigma_A > \sigma_D$, and in the region below and to the right of the $\sigma_A = \sigma_D$ line, we find $\sigma_D > \sigma_A$. We see in Figs. 3 and 4 that the experimental points lie somewhat below the $\sigma_A = \sigma_D$ magnetization curve. However, these observed deviations are viewed as being in good agreement with molecular-field theory, considering the approximate nature of this treatment. The important feature of the data is that the reduced internal fields for each sublattice are essentially the same. Thus, the values of α and δ which apply to these alloys must lie very close to the $\sigma_A = \sigma_D$ line of Fig. 5. We can obtain further limitations on the values of α and δ from the following considerations.

From the distances between the various types of Fe atoms, we would expect that the exchange energy J_{AD} of A and D atoms would be the largest and that between D atoms, J_{DD} , would be the smallest, but still positive. That is, we expect $J_{AD} > J_{AA} > J_{DD} > 0$. If molecular-field theory is applicable, we might also expect that J_{AD} would be somewhat less than the exchange energy for

TABLE II. Exchange energies in $^{\circ}\text{K}$ for Fe_3Al and Fe_3Si .

	J_{AD}	J_{AA}	J_{DD}
Fe_3Al	120 ± 15	70 ∓ 20	7 ∓ 5
Fe_3Si	145 ± 15	80 ∓ 20	8 ∓ 5

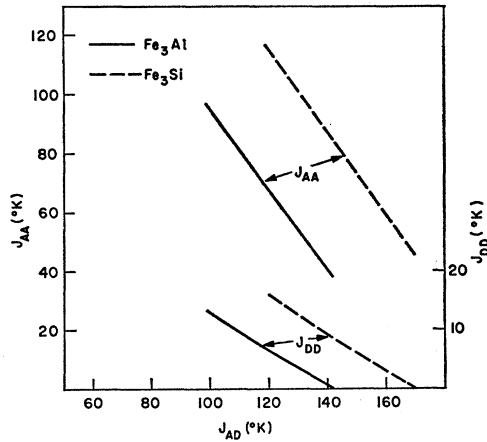


FIG. 7. Sublattice and interaction exchange energies for the ordered Fe_3Al and Fe_3Si structures. The abscissa gives the interaction exchange energy J_{AD} in $^\circ\text{K}$. For a given J_{AD} , read J_{AA} and J_{DD} from the left and right ordinate axis, respectively.

pure Fe. Using the same definition of J as given in Ref. 3b, the molecular-field coefficients and exchange energies are related by

$$\lambda_{AD} = 2z_{AD}J_{AD}/N_D g_A g_D \mu_B^2, \quad (7)$$

with similar expressions for λ_{AA} and λ_{DD} . Here $N_D = \frac{1}{3}N$. Z_{AD} is the number of D -type atoms surrounding an A type atom. We thus find that the region of α , δ values which satisfies the above restrictions is $0 < \delta < 0.45$ and $0.2 < \alpha < 0.75$. Since T_C is known for both alloys, we obtain a further relation between the molecular-field coefficients from Eq. (6). From all these considerations, we can obtain values of the molecular-field coefficients and through Eq. (7), the exchange energies. Figure 7 shows these exchange energies. Here, we have plotted J_{AD} in $^\circ\text{K}$ along the abscissa and the values of J_{AA} and J_{DD} along the left and right ordinate axes; all

values are positive. In Table II, we list the estimates obtained for the exchange energies of both Fe_3Al and Fe_3Si . The $+$ and $-$ signs vary in the directions indicated in the table, i.e., when J_{AD} increases, J_{AA} and J_{DD} decrease. The values obtained for the exchange energies are very reasonable, considering that the value for pure Fe is 160°K .⁹

Thus, we obtain a satisfactory agreement between the molecular-field theory and the experimental results—much better, in fact, than would be anticipated in most metallic systems. The reason for the good agreement is believed to be the following. In many aspects, the behavior of these alloys is very similar to that of pure Fe. Previous experiments⁷ have indicated that a Ruderman-Kittel-Kasuya-Yosida-type interaction of the $4s$ conduction electrons is not responsible for the ferromagnetism in Fe (in fact, their behavior would lead to antiferromagnetism). Thus, the ferromagnetic behavior is thought to be due to the itinerant d -like electrons. Suppose that the itinerant ones among the d electrons are very few in number and therefore have only a small extent in k space. Then the oscillations in their polarization will be of long range, perhaps over four to five nearest neighbors. This slow variation of exchange coupling over many neighbors will ensure approximate validity of the molecular-field treatment. The success of molecular-field theory is thus consistent with the view that the ferromagnetism of Fe and these alloys is due to the long-range coupling of the atomic spins by the itinerant d electrons.

ACKNOWLEDGMENTS

The author would like to thank S. S. Wilson for his aid throughout this experiment and the Physics Division of the Aspen Institute for Humanistic Studies for their hospitality while writing this paper.

⁹ P. R. Weiss, Phys. Rev. **74**, 1493 (1948).